Fourth International Conference on FRP Composites in Civil Engineering (CICE2008)
22-24 July 2008, Zurich, Switzerland

Numerical prediction of shear crack angles for FRP shear-strengthened concrete beams

A. Godat, P. Labossière & K.W. Neale
University of Sherbrooke, Sherbrooke, Quebec, Canada

ABSTRACT: The shear crack angle is a key parameter in the calculation of the FRP contribution to the shear capacity of a strengthened concrete beam. A non-linear finite element model has been developed to simulate the behavior of six beams grouped in three series according to their dimensions. One un-strengthened beam of each series was used as a benchmark and its behavior was compared to that for a beam strengthened with U-wrap jackets. It was found that the numerical model is able to successfully simulate the characteristics of the shear-strengthened beams. The numerical predictions compare very well with the experimental data in terms of load–deflection relationships. The analysis of the slip profiles along the FRP strip is helpful for understanding the bond behavior between the concrete and FRP strips. The interfacial slip profiles are used to predict the crack formation angle along the shear span, and these predictions agree very well with the experimental measurements. The numerical results give failure modes that are identical to those obtained experimentally.

1 INTRODUCTION

Extensive research results show that FRPs display excellent performance in comparison to the conventional strengthening techniques. With the development of the technology of upgrading existing structures with FRPs, a number of issues related to structural behavior have been identified (Neale 2000). The bonding of external FRP stirrups is considered a promising method to increase the shear capacity.

In comparison to analyses on FRP flexural strengthening, theoretical investigations concerning the behavior of reinforced concrete beams strengthened in shear with FRP composites are rather limited. The numerical studies on FRP shear-strengthened beams include those of Kaliakin et al. (1996), Arduini et al. (1997), Malek and Saadatmanesh (1998a,b), Al-Mahaidi et al. (2001), Wong (2001), Lee (2003), Godat et al. (2007a,b). In general, the numerical simulations provided quite satisfactory predictions of the overall behavior of the shear-strengthened beams, in particular in terms of the overall load–deflection curves. However, most of these analyses did not explicitly address the details of the FRP/concrete interface and less attention has been paid to investigate the slip profiles along the FRP strip depth.

In this investigation, the finite element model focused on the FRP/concrete interfacial responses and was capable of simulating the debonding failure modes. In order to verify the accuracy of the numerical model, various sizes of CFRP shear-strengthened beams were considered. The accuracy of the numerical model was evaluated by comparing predictions to experimental results. Once the accuracy of the analysis was established, numerical studies were carried out to investigate complex mechanisms that are difficult to characterize experimentally, such as the interfacial slip profiles and shear crack angles.

2 FINITE ELEMENT MODEL

A three-dimensional finite element program, ADINA (2005), was utilized for the numerical analysis. In the analysis, appropriate material models were employed to represent the behavior of the concrete, the steel reinforcement, and the CFRP strips. These are described in detail in the ADINA theory and modeling guide (ADINA 2005). A hypoelastic constitutive model is used to characterize the concrete behavior. In addition, to model the bond behavior at the FRP/concrete interface, interface elements that are able to properly represent the local shear–slip characteristics and failure were selected (Fig. 1). The details of the constitutive models and their implementation into the numerical analysis are described in detail in Godat et al. (2007a; 2007b). The nonlinear load–deformation behavior of the structure is simulated under displacement-controlled loading conditions, as was the case in the experiments.

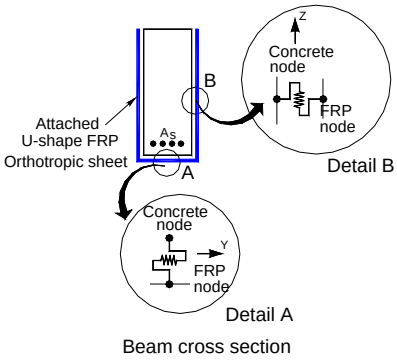

Figure 1. Finite element model.

The cases analyzed correspond to the specimens tested by Qu et al. (2005). This involved three series of reinforced concrete beams. Each series included a reference beam and a CFRP U-jacket strengthened beam. The reference beams are labeled by the letters RC, followed by a number that denotes the series. The notations U4, U5 and U6 indicate the U-jacket strengthened beams for the first, second and third series, respectively. The flexural reinforcement bars, having a with yield strength of 400 MPa, were installed only on the bottom. No steel stirrups were placed in the shear span of interest (right shear span); however, sufficient steel stirrups were installed in the other span (left shear span) to ensure that failure would occur in the shear span of interest. All beams were simply supported and subjected to a monotonic static loading applied at the center of the beam. Table 1 lists the dimensions of the specimens along with their material properties. In Table 1, a represents the shear pan length, whereas s_f denotes the clear distance between the CFRP strips. Five CFRP strips were installed along the shear span length and were numbered sequentially beginning from the support.

Table 1. Geometrical dimensions and material properties of the tested beams

Beams series	Spec.	Beam dimensions (mm) L	b	h	a (mm)	Number of long. steel	Concrete (MPa) f_c'	f_t	CFRP dimensions t_f (mm)	w_f (mm)	s_f (mm)
First series	RC1	900	100	200	340	6ϕ12	51.2	2.55	—	—	—
	U4						51.2	2.55	0.111	30	20
Second series	RC2	1800	200	400	680	6ϕ25	49.7	2.93	—	—	—
	U5						51.2	2.93	0.222	60	40
third series	RC3	2700	300	600	1020	6 ϕ32 + 3ϕ25	50.5	3.16	—	—	—
	U6						51.0	3.16	0.333	90	60

3 NUMERICAL RESULTS AND DISCUSSION

The results presented in the following sections are in terms of the ultimate load carrying capacities, load–deflection relationships at the centre of the beam, and failure modes. Special emphasis is placed on the slip profiles at the interface between the concrete and CFRP strips.

3.1 *Load–deflection relations and failure modes*

Table 2 presents a comparison between the numerical predictions and the experimental results for the various specimens. As can be seen in this table, for the control specimens the predicted ultimate carrying capacities are 4%, 5% and 2% greater than the test values for the RC1, RC2 and RC3 beams, respectively. The predicted failure modes were identical to the experimental observations. The numerical predictions of the ultimate load carrying capacities for the strengthened beams were 105 %, 101% and 102% of the estimated experimental values for the U4, U5 and U6 beams, respectively. In addition, the proposed model successfully simulated the failure mode of the CFRP U-strips. Debonding of the CFRP U-jacket strips was the dominant failure mode, which is indeed the corresponding experimental failure mode. The position of the first delamination of the interface elements corresponds to the maximum slip values, which will be discussed in the following section. The delamination progressed until crushing of the concrete.

Table 2. Experimental and numerical results

Beams sets	Spec.	Experimental results		Numerical results		$\frac{P_{num.}}{P_{exp.}}$	Failure modes	
		Max. load (kN)	Max. def.[a] (mm)	Max. load (kN)	Max. def. (mm)		Experimental	Numerical
First set	RC1	160	1.9	166	1.8	1.04	concrete crushing	concrete crushing
	U4	203	2.2	213	2.1	1.05	debonding	debonding
Second set	RC2	709	3.6	745	3.3	1.05	concrete crushing	concrete crushing
	U5	809	4.2	813	3.9	1.01	debonding	debonding
Third set	RC3	1626	6.6	1659	6.1	1.02	concrete crushing	concrete crushing
	U6	2018	6.5	2053	6.4	1.02	debonding	debonding

Figures 2(a) and 2(b) present the comparisons between the experimental and numerical results in terms of the load–deflection relationships of the tested beams of the first and the second series, respectively. The numerical models were able to simulate the load–deflection relationships. In view of the displacement-controlled solution adopted in our analysis, it was possible to simulate the post-peak behavior. The numerical load–deflection curves were almost similar to the experimental ones before cracking occurred. It is observed that the numerical analysis slightly overestimates the stiffness behavior in the cracking region. The numerical predictions underestimate the deflection corresponding to the maximum load, but the results are within a reasonable range of the experimental values. Thus, the proposed numerical model proved its ability to predict the load–deflection relationships with high accuracy. Besides, the model led to failure modes identical to those observed experimentally.

3.2 *Slip profiles along the FRP-concrete interface and shear crack angles*

In view of the good agreement between the numerical and experimental results in terms of the load–deflection behavior, the numerical model is expected to provide valuable insight into aspects of the interfacial behavior that are very difficult to assess experimentally. The interfacial slip profiles were thus used to predict the crack formation angle along the shear span. It can generally be stated that in the experimental program shear cracks propagated as the load increased and failure occurred due to debonding of the FRP strips over the main diagonal shear crack. This debonding leads to an instantaneous increase in the vertical strains of the bonded CFRP strips. As far as the interfacial slip behavior of the strengthened specimens is concerned, it can be concluded that the crack inclinations resemble the measured crack angles.

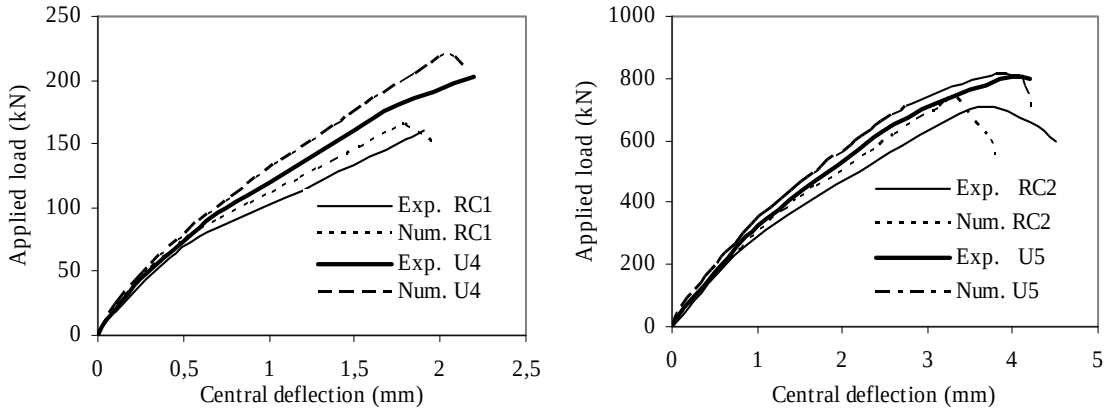

(a) (b)

Figure 2. Load–deflection relationships: (a) first series, and (b) second series.

For the strengthened specimens, the values of the maximum slip are computed using the Lu et al. relations (2005). These are 0.24 mm, 0.23 mm and 0.22 mm for the strengthened specimen of the first, second and third specimen, respectively. (Figures 3(a)-3(e) show the slip profiles along the interface for the U-jacket strengthened specimen U4. The predicted slip profiles for the CFRP strip closest to the applied load, F5, is presented in Fig. 3(a). At a low load level ($52kN$), the interfacial slip is concentrated around the middle of the beam depth and decreases towards the ends of the beam. As the applied load is increased up to the cracking stress, the interfacial slip increases with maximum values moving to the top end of the strip. The presence of the cracks influences the behavior of the slip profile by fluctuating the values from negative to positive. With an increase of the applied load, the shear cracks propagate and the slip values increase correspondingly. As a result, the slip profile increases dramatically in the region near the vicinity of the applied loads, thus causing debonding of that strip, F5.

The overall evolution of the interfacial slip profiles predicted for the next strip from the applied load, F4, is presented in Fig. 3(b). These are consistent with the behavior of the previous strip, F5. The slip distributions show that the maximum slip values occur at 50 mm below the top edge of the CFRP strips. The debonding initiates at the point of the maximum slip value and propagates towards the top end of the CFRP strip. At the same load levels, the strip F5 shows higher slip values than does the strip F4. This indicates that the delamination initiates in the strip closest to the applied load and propagates towards the support.

Figure 3(c) shows the slip profiles along the strip depth for the third strip, F3, placed midway along the shear span. Clearly, before crack initiation, small slip values are predicted around the mid-depth of the CFRP strip. The abrupt increase of the slip values around the mid-depth was due to a local effect caused by the shear crack. In this case, delamination initiates at the position of the maximum interfacial slip, leading to eventual failure towards the top edge. For the last two CFRP strips, F2 and F1, the slip profiles are plotted in Figs. 3(d) and 3(e), respectively. It can be observed that the maximum values of these slip profiles concentrate at a distance 50 mm and 25 mm from the bottom end of the strip, respectively. Furthermore, the interfacial slip values decrease towards the top ends of the CFRP strips.

The shear crack angle is a key parameter in the calculation of the FRP shear resistance capacity. In Figs. 4(a) and 4(b), the formations of the shear cracks in the experimental tests for the strengthened beams of the first and the second series are depicted, respectively, and the crack angles are illustrated. As seen in Figs. 4(a)-4(b), the strengthened beams show typical inclination cracks. The maximum slip value of the first strip adjacent to the applied load was observed at the top edge; however, the higher slip values of the CFRP near the support were measured at the bottom edge of the CFRP strip. Consequently, this means that the connection of the points of the ultimate interfacial slip values can be considered as an indication of the crack inclination angle. As indicated in Fig. 4(a), the crack angle of the strengthened specimen U4 was $32°$. In the numerical model, the inclination angle between the maximum slip values varied. Overall, the average angle of the maximum slip values, which represents the crack angle,

was $28°$. This result shows that the predicted crack angle of the numerical model is in very good agreement with the experimental data.

The previous analysis for the first series was repeated for the strengthened specimen of the second and the third series. The experimental reported shear crack angles for the strengthened specimens of the second and the third series were $33°$ and 34^o, while the numerical model predicted shear cracks with angles of 36^o and 28^o, respectively. The predicted results support the conclusion that the numerical model is representative of the experimental behavior.

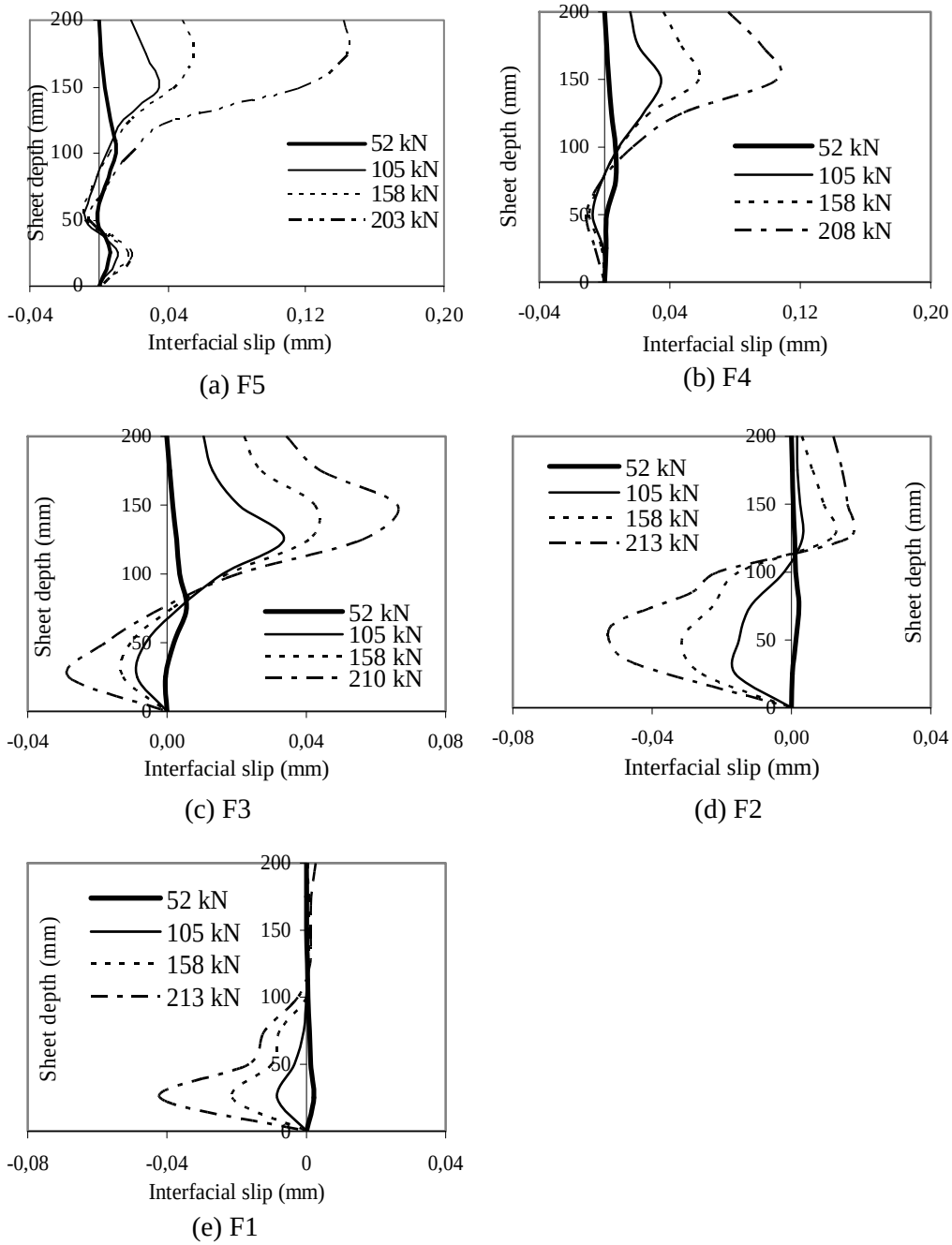

Figure 3. Interfacial slip profiles along the FRP depth of the bonded strips for specimen U4.

4 CONCLUSION

Numerical modeling was carried out to investigate the behavior of FRP shear-strengthened beams. A nonlinear constitutive model was incorporated to represent the interfacial behavior between the concrete and CFRP strips. The comparison between the numerical predictions and experimental results presents excellent agreement in terms of the ultimate load carrying capacities, load–deflection relationships, and failure modes. Based on the numerical results, the following conclusions are drawn:

- Accounting for the slip profiles along the CFRP depth is necessary to assess the debonding phenomena.
- A consistency is observed between the shear crack locations and the maximum values of the interfacial slips; the delamination occurs over the main diagonal shear crack.
- The numerical model is able to capture the shear crack angle along the shear span.

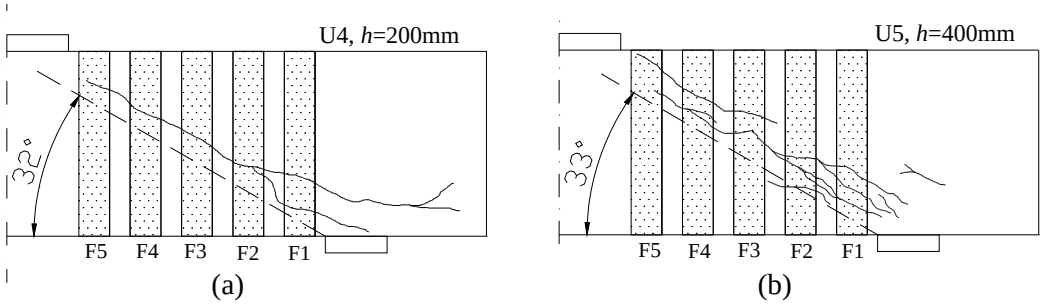

Figure 4. Experimental shear crack inclination angles for the strengthened specimen: (a) first series, and (b) second series.

5 REFERENCES

ADINA 2005. *Theory and Modeling Guide*, Vol. 1, Chapter 3, Version 8.3. ADINA R&D Inc., Watertown, MA, USA.

Al-Mahaidi, R., Lee, K., and Taplin, G. 2001. Behavior and analysis of RC T-beams partially damaged in shear and repaired with CFRP laminates. *Proc. 2001 Structural Congress and Exposition*, ASCE, P.C. Chang, Ed., May 21–23, Washington, DC.

Arduini, M., Nanni, A., Di Tommaso, A., and Focacci, F. 1997. Shear response of continuous RC beams strengthened with carbon FRP sheets. *Non-Metallic (FRP) Reinforcement for Concrete Structures*, Proc. 3rd Int. Symposium, Vol. 1, Japan Concrete Institute, Tokyo, Japan, 459-466.

Godat, A., Neale, K.W., and Labossière, P. 2007a. Numerical modeling of FRP shear-strengthened reinforced concrete beams. *Journal of Composites for Construction*, ASCE 11(6), 640-649.

Godat, A., Neale, K.W., and Labossière, P. 2007b. Towards modelling FRP shear-strengthened reinforced concrete beams.'' *Fiber Reinforced Polymer Reinforcement for Concrete Structures*, T.C. Triantafillou, Ed., University of Patras, Greece, 10p.

Kaliakin, V. N., Chajes, M. J., and Januszka, T. F. 1996. Analysis of concrete beams reinforced with externally bonded woven composite fabrics. *Composites Part B: Engineering*, 27(3-4), 235-244.

Lee, T. K. 2003. *Shear strengthening of reinforced concrete T-beams strengthened using carbon fibre reinforced polymer (CFRP) laminates*. Ph.D. Thesis, Department of Civil Engineering, Monash University, Victoria, Australia.

Malek, A., and Saadatmanesh, H. 1998a. Ultimate shear capacity of reinforced concrete beams strengthened with web-bonded fiber-reinforced plastic plates. *ACI Structural Journal*, 95(4), 391-399.

Malek, A., and Saadatmanesh, H. 1998b. Analytical study of reinforced concrete beams strengthened with web-bonded fiber reinforced plastic plates or fabrics. *ACI Structural Journal*, 95(3), 343-352.

Neale, K.W. 2000. FRPs for structural rehabilitation: a survey of recent progress. *Progress in Structural Engineering and Materials*, 2(2), 133-138.

Qu, Z., Lu, X.. Z., and Ye, L. P. 2005. Size effect of shear contribution of externally bonded FRP U-jackets for RC beams. *Bond Behaviour of FRP in Structures* (BBFS 2005), Proc., Int. Symposium, J.F. Chen and J.G. Teng, Eds., International Institute for FRP in Construction, Hong Kong, China, 363-371.

Wong, R. 2001. *Towards modelling of reinforced concrete members with externally bonded fibre reinforced polymer (FRP) composites*. M.Sc. Thesis, Civil Engineering Department, University of Toronto, Toronto, Ontario.